uS

FACULTY OF SCIENCE AND TECHNOLOGY
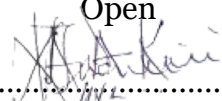
MASTER THESIS

Study programme / specialisation:
Marine and Offshore Technology

The spring semester, 2022

Open

Author: John Anani Kadiri

....
(Signature author)

Course coordinator: Professor Yihan Xing

Supervisor(s): Professor Yihan Xing

Thesis title: Determining operating envelope for blade on a floating wind turbine using the extreme value ACER method

Credits (ECTS): 30

Keywords: Wind Turbine, ACER method

Pages: 25

Stavanger, 13th June 2022

SUMMARY

A method to predict extreme loads adequately and accurately on the blades of a 10 MW large floating wind turbine with the objective of creating solutions for inspection in the most extreme weather conditions characterized by a reference wind speed of 16 m/s as a practical step towards achieving a larger maintenance window and further reduction in operations and maintenance (O & M) cost is proposed in this report.

The method being proposed is the Average Conditional Exceedance Rate (ACER)[1] It is described as a method where extreme values can be predicted based on a sampled time series. It is further explained that the method is mainly structured to justify statistical dependency among the sampled data points accurately. Veritably, if accurately operated, statistical estimates of the exact extreme value distribution provided by the data in most cases of practical interest would be produced. The problem of having to declutter the data to establish autonomy, which is a preconditioned component in the application of, for example, the ideal peaks-over-threshold method, is avoided. The proposed method also targets the use of sub asymptotic data to enhance the veracity of the prediction[2]. In this paper, the method would be demonstrated by application to hindcast data.

FORWARD

In this scientific research, a methodological study has been carried out to compare the extreme loads on the blades of a 10MW floating wind turbine. A systematic comparison is being made between a probabilistic method (Gumbel) and ACER (Average Conditional Exceedance Rate) and conclusions made on what results to be trusted in terms of the confidence interval using MATLAB.

Where results are found satisfactory, it is proposed that maintenance windows during harsh weather could be increased because when adequately predicted to a high degree of certainty, remotely operated vehicles could be designed for maintenance operations with adequate strength and dexterity to withstand extreme weather.

A significant part of the cost of maintenance occurs when wind technicians wait for the right weather window to perform maintenance operations, therefore with the annual growth in the installation of offshore wind turbines, this report poses to be a significant study for industry professionals, operators, and service companies.

I'm thankful to have had this learning experience with Prof. Yihan Xing who gave adequate support through this project.

Contents

Table of figures

1. INTRODUCTION:

1.1 Background:

Based on the latest review by the International Energy Agency (IEA), Norway's energy policies have created a sustainable management of its significant hydrocarbon resources and revenues. Nonetheless, as the world looks on cutting down its reliance on fossil fuels[3], wind energy has become a mainstream energy source for power generation with an important role to play in the world's energy market[4].

According to the International Renewable Energy Agency (IRENA), increased deployment of wind power would contribute to more than one-quarter of the total emission reductions needed by 2050 to set the world on an energy pathway towards achieving the Paris climate targets[5].

Offshore wind farms (OWF) comprise of a number of wind turbines. A wind turbine consists of three main components: the tower, a nacelle or the generator house, and the rotor. The rotor is comprised of three blades connected to a central hub on the nacelle.

The development of OWF's, operations and maintenance are highly dependent upon reliable information on wind conditions[6]. Incoming turbulent wind affects all components above the water surface and the aerodynamic loads from the rotor are critical but drag forces on the tower and support structure (assumed to be equivalent to the wind velocity squared) can be significant in extreme conditions when the rotor is parked[7]. Parked rotor is referred to here as the operational condition of our investigation.

A significant part of the cost of maintenance occurs when wind technicians wait for the right weather window to perform maintenance operations. When extreme wind speeds occur, and the

rotor is parked (maintenance position) loads are created on the blades[8]. The importance of evaluating and predicting the wind speeds and the blades response correctly, becomes very important.

To evaluate extreme wind turbine loads, one or two of the following distinct methods can be applied. The first method comprises of executing a simulation for rare occurrences that lead to high structural loads, while with the second method, the wind turbine is simulated during normal operating conditions. Further, is an extrapolation of the results with a probability distribution and analysis of the extreme tail. There is a requirement by the IEC61400-1 standard that both approaches should be combined in obtaining extreme design loads[9].

1.2 State of the Art

Today, the ACER method makes use of a broad range of parametric functions to extrapolate extreme value distribution tail, its estimation of extreme wind speeds is not dependent on unambigous assumption of asymptotic distribution type, while the latter is a key assumption in Gumbel as analyzed in this work The approach of a given value as an expression containing a variable which tends to infinity is usually unverifiable exclusively on the bases of a agiven data set, therefore there is a level of convenience related to the asymptotic assumtion.[10] Recently developed methods for estimating extreme wave statistics are discuessed in this report.

1.3 Limitations

Evaluating the extreme wind turbine loads did not pose much of a challenge as the hindcast data was available as well as the relevant software for the post processing and analysis of the data.

ACER which is also a MATLAB component was available in short notice.

Nonetheless, there's a significant difference to be on site, take measurement as compared to when working on such projects having a picture of the entire set up in the mind.

The author has generally found it a very interesting learning experience, where the use of software tools like MATLAB that were employed briefly during the MSc. in Marine and Offshore Technology at the University of Stavanger, were used extensively in this work and this has given a better command of the use of the software.

2. SYSTEM DESCRIPTION

A FWT (Floating Wind Turbine) system of 10-MW [11] illustrated in Figure 1 would be used in this report. The following sections will discourse the reference wind turbine and its components, including properties of the nacelle, rotor, and blades.
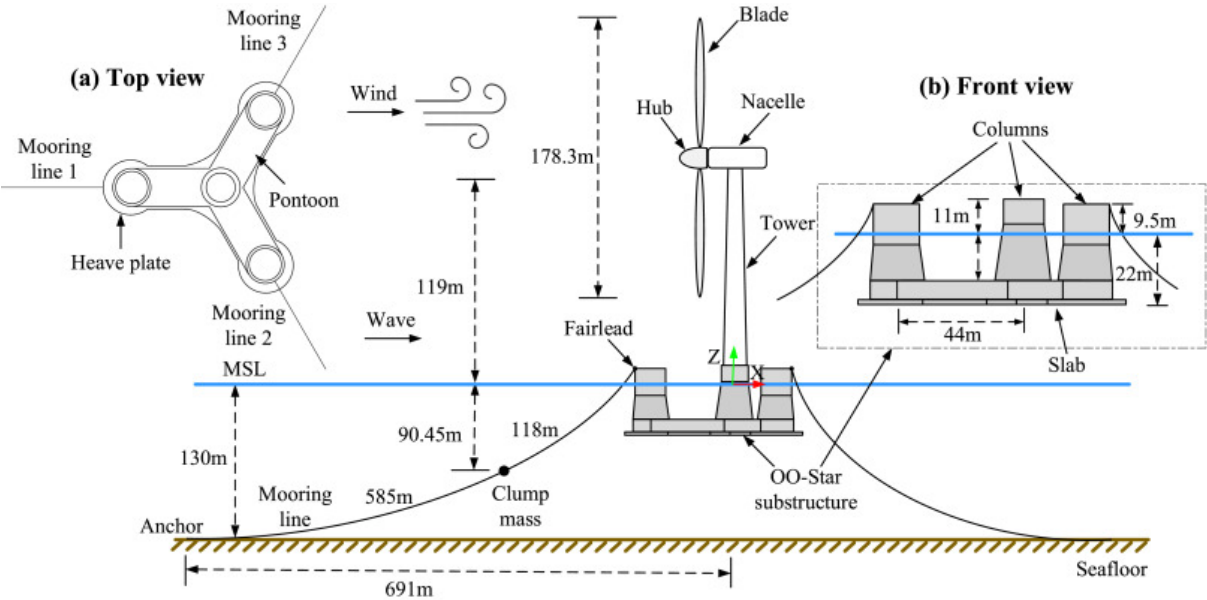
Figure 1 Sketch of the OO-Star Wind Floater Semi 10-MW concept[12]

2.1 DTU 10-MW Reference Wind Turbine

The DTU 10-MW reference wind turbine's (RWT) [13] design was from the NREL 5-MW RWT which was according to the International Electrotechnical Commission (IEC) a Class 1A wind system. It is traditionally equipped with three blades partitioned into 100 regions radially and 10 regions circumferentially and equipped with a variable speed and collective pitch control system. Several academic works have undertaken the study and development of the DTU 10-MW RWT, an example is Wang et al.[14] amongst others. Table 1 depicts a summary of the DTU 10-MW RWT.

Table 1 Essential parameters of the DTU 10-MW reference wind turbine[11]

Parameter	Value
Rating	10-MW
Type	Upwind/3 blades
Control	Variable speed, collective pitch
Drivetrain	Medium-speed, multiple stage gearbox
Cut-in, rated and cut-out wind speed (m/s)	4, 11.4, 25
Minimum and maximum rotor speed (rpm)	6.0, 9.6
Maximum generator speed (rpm)	480
Rotor diameter (m)	178.3
Hub height (m)	119.0
Rotor mass (kg)	227962

Nacelle mass (kg)	446036
Tower mass (kg)	1.257×10^6

2.2 OO-Star Semi-submersible Wind Floater and Mooring System

Dr. techn. Olav Olsen AS initiated the semi-submersible floating structure in the LIFES 50+ project [11] to support the 10-MW RWT used in this work. The floater hosts a central column with three outer columns encompassing post-tensioned concrete. A star shaped pontoon seats the four columns with a slab imbued at the bottom. The floater is kept in position with three catenary mooring lines, and a clumped mass is attached to each line separating the lines in two segments.

Table 2 Properties for the OO-Star Wind Floater Semi 10-MW floating substructure[12]

Parameter	Value
Water depth (m)	130
Draft (m)	22
Main material	post-tensioned concrete
Overall mass ($\times$ 1000 kg)	21709
Displaced volume (m3)	23509
Tower base interface >mean sea level (m)	11
Center of mass location < mean sea level (m)	15.255

Center of buoyancy location<mean MSL (m)	14.236
Roll & pitch inertia about CoM (kg, m^2)	9.43×10^9
Yaw inertia about center of mass (kg, m2)	1.63×10^{10}

Figure 2 Main characteristics of the OO-Star floater of the 10-MW wind turbine[11]

Table 3 Properties for the OO-Star Wind Floater Semi 10-MW floating substructure[12]

Parameter	Value
Water depth (m)	130
Draft (m)	22

Main material	post-tensioned concrete
Overall mass (× 1000 kg)	21709
Displaced volume (m3)	23509
Tower base interface >mean sea level (m)	11
Center of mass location < mean sea level (m)	15.255
Center of buoyancy location<mean MSL (m)	14.236
Roll & pitch inertia about CoM (kg, m^2)	9.43×10^9
Yaw inertia about center of mass (kg, m2)	1.63×10^{10}

Table 4 Elements of the mooring system of the 10-MW FWT [12]

Parameter	Value
Radius to anchors from platform centerline (m)	691
Anchor position below MSL (m)	130
Initial vertical position of clump mass below MSL (m)	90.45
Initial radius to clump mass from centerline (m)	148.6
Length of clump mass upper segment (kg)	118
Length of clump mass lower segment (kg)	585

Equivalent weight per length in water (N/m)	3200.6
Extentional stiffness (N/m)	1.506×10^9
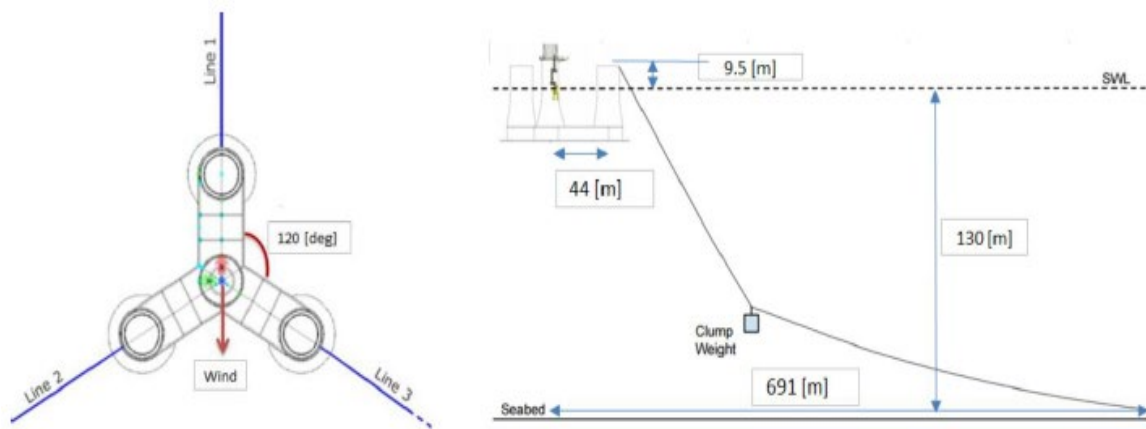
Figure 3 Sketch of the mooring system in the 10-MW FWT (left: top view; right: side view) [11]

A dynamic representation of the 10-MW floating -type floating wind turbine, also established in SIMA is shown in Figure 3[15]. The hull, hub and nacelle are treated as rigid objects in this model, although the blades, tower and shafts modelled by non-liner beam elements are classified as flexible bodies. A single DOF (Degree of Freedom) torsional spring-damper system is the bases for the modelling of the drive train. Nonlinear bar elements are used to model the mooring lines considering axial stiffness alone. As compared to the monopile model, the BEM method is also used to calculate the aerodynamic loads.

3. METHODOLOGY

A time domain entirely coupled aero-hydro-servo-elastic simulation tool SIMO-RIFLEX, developed by SINTEF is used to numerically model the 10-MW semi-submersible type floating wind turbine (SSWT). Rigid body hydrodynamic loads on the floating structures are calculated with SIMO[16]. The dynamic response of the flexible elements inclusive of the aerodynamic loads is based on the Blade Element Momentum (BEM) theory. Java is used to script the external controller for the control of the generator torque and blade pitch. Omberg et al.[17] and Luxcey et al.[18] have verified the SIMO-RIFLEX wind turbine module and it has been applied in the OC5 project[19].

3.1.1 Aerodynamics

In the recent state-of-the-art, computational fluid dynamics (CFD) analysis and Blade Element Momentum (BEM) based models are used to analyze and design a wind turbine blade. CFD code simulations are accurate but very time consuming. Alternatively, codes based on BEM are fast, but have some limitations[20]. The BEM theory relies on the premise that there are no aerodynamic interactions between different blade elements and the forces on the blade elements are solely determined by the lift and drag coefficients[21]. The Prandtl and Glaurt corrections, dynamic stall, tower shadow, and skewed wake corrections are calculated with a nonlinear finite element solver[22] which also provided the link to an external controller.

3.1.2 Hydrodynamics

The Morrison's equation is the bases for the evaluation of the hydrodynamic loads acting on the semi-submersible floater where a potential flow theory addresses wave pressures and viscous loads. Added mass, potential damping coefficients and first order wave excitation load transfer functions are initially estimated in a frequency domain using a panel code,

WAMIT[23]. The transformation of the hydrodynamic coefficients from frequency to time domain done through a method of yield derivative estimation for nondifferentiable or truncated probability-density functions (PDFs) is proposed and applied to yield optimization. Convolution technique is applied and based on perturbation approach. It requires a minimal number of samples per yield-optimization-algorithm step as it constructs some approximation to the original PDF[24].

3.1.3 Structural dynamics

Integrated numerical tools have been developed by companies and research institutions to meet the challenge of the increased complexity of the design, modelling and analysis of the FWT because of the combination of structural, hydrodynamics and aerodynamics. Among these codes, the SIMO software developed by MARINTEK has been used in this work to model the specific wind turbine as a system of rigid bodies in the time domain. The ensuing total motion, structural shear forces and generated power will be compared[18].

3.1.4 Control system dynamics

The functionality of the 10-MW FWT's control system varies with respect to its changing operational modes. The modes are classified into below-rated or full-rated sector. The generator torque-speed curve drives the circumvolutory speed of the rotor uniform to the highest tip speed ratio, permitting the turbine to reach its ultimate power in the below-rated sector. At the full rated sector, the blade pitch is adapted using a proportional-integral (PI) algorithm for the control of the circumvolutory speed of the rotor to keep the generation of rated power for speeds higher than the FWT's rated speed. To avert the adverse damping effects detrimental to the FWT's the PI parameters employed differ from those in land based RWT[25].

3.2 Extreme value prediction

Evaluations of the risks of extreme weather events, like high wind velocities require processes to statistically evaluate their return periods from measured data[26]. It is therefore crucial for the safety and economically optimized engineering of wind turbine blades to estimate the changes in the wind speed and analyzing the blade response in park mode. The extreme value in any stochastic process Y(t) appropriated through a period (T), is classified as the highest maxima extracted form a set of distinctive maxima.

$$Y_e = \max\{Y_{m1}, Y_{m2}, Y_{m3}, Y_{m4} \dots \dots, Y_{mn}\}, \qquad i = 1, \dots, n \quad (1)$$

Y_e depicts the highest maximum value and Y_{mi} describes the individual maxima. Consequently, it is seen that the individual maxima are independently and identically distributed across the common distribution function $F_{ym}(y)$. Therefore, the distribution of Y_e is labelled from the equation below as:

$$F(y) = \mathbf{Prob}\{Y_e \le y\} = [F_{Ym}(y)]^n, \qquad i = 1, \dots, n \quad (2)$$

In approximating extreme value distribution, a combination of different statistical methods has been employed. Examples of extreme value methods used in the study of wind turbines includes an evaluation of extreme structural responses in a floating vertical axis wind turbines by Madsen et al.[27] and extreme responses due to wave nonlinearity on a semi-submersible floating wind turbine by Zhang et al.[28]. ACER and Gumbel methods are used in this paper.

3.3 ACER (Average Conditional Exceedance Rate)

The estimation of extreme structural responses is carried out by ACER method in this paper. Gaidai et al. [29] proffered this method which is derived for a discretely sampled response process. The basis for calculating the exceedance probability for extreme value approximation

is a series of conditional approximation. The main purpose of the ACER method is to resolve the distribution of extreme value without error, expressed as:

$Q_N = \max\{Y_s, \dots, N\}$. Let $P_\eta = \text{Prob}(Q_N \leq \eta)$ stand for the probability of the occurrence of the extreme equivalent η resulting to:

$$P_\eta = \text{Prob}(Q_N \leq \eta) = \text{Prob}(Y_1 \leq \eta, \dots, Y_\eta, \dots, Y_N \leq \eta) \qquad (3)$$

A torrent of conditional approximation $P_k(\eta)$ is employed for the effective solution of the above equation, as k increases $P_k(\eta)$ leans towards P_η. For $N \gg 1$ and $k = 1,2, \dots P_k(\eta)$ is depicted as:

$$P_k(\eta) \approx \exp\left(-\sum_{S=k}^{N} \propto_{ks}(\eta)\right) \qquad (4)$$

where $\propto_{ks}(\eta) = \text{Prob}(Y_1 > \eta | Y_{s-1} \ll \eta, \dots, Y_{s-k+1} \leq \eta)$, it also expresses the exceedance probability conditional on $k-1$ preceding non-exceedances.

Equation (4) is evaluated following ACER, expounded as:

$$\varepsilon_k(\eta) = \frac{1}{S-k+1} \sum_{s=k}^{N} \propto_{ks}(\eta), k = 1,2, \dots \qquad (5)$$

$\tilde{\varepsilon}(\eta)$ is used in place of $\varepsilon_k(\eta)$ for $k \geq 2$ for convenience in using long term statistics, formularized as:

$$\tilde{\varepsilon}(\eta) = \lim_{n \to \infty} \frac{\sum_{s=k}^{N} \propto_{ks}(\eta)}{S-k+1} \qquad (6)$$

$\propto_{ks}(\eta)$ depicts the executed values for the surveyed time series, and $\lim_{n \to \infty} \frac{\sum_{s=k}^{N} \propto_{ks}(\eta)}{S-k+1} = 1$.

The sample valuation for the ACER in stationary and nonstationary time series is connoted as:

$$\tilde{\varepsilon}(\eta) = \frac{1}{B} \sum_{V=1}^{B} \tilde{\varepsilon}^{(V)}(\eta) \qquad (7)$$

B depicts the number of samples, and

$$\tilde{\varepsilon}^{(V)}(\eta) = \frac{\sum_{s=k}^{N} \propto_{ks}{}^{V}(\eta)}{S-k+1} \qquad (8)$$

V depicts the realization number.

If there are enough independent realizations, a confidence interval (CI) of 95% for the ACER can be evaluated with:

$$CI(\eta) = \tilde{\varepsilon}(\eta) \pm \frac{1.96^{\hat{D}_k(\eta)}}{\sqrt{B}} \qquad (9)$$

$\hat{D}_k(\eta)$ represents the standard deviation of samples and is evaluated by:

$$\hat{D}_k(\eta)^2 = \frac{1}{B-1}\sum_{V=1}^{B}(\tilde{\varepsilon}^{(V)}(\eta) - \varepsilon_k(\eta))^2 \qquad (10)$$

Direct numerical simulations are the bases for the equations above in evaluating the average exceedance rate. The computational time can be reduced by extrapolation.

Infer that the mean exceedance rate in the tail performs equivalently to

$\exp\{-w(\eta - x)^y\}(\eta \geq \eta_o \geq y)$, where w, x and y are constants.

The ACER is then expressed as:

$$\varepsilon_k(\eta) \approx z_k(\eta)\exp\{-w_k(\eta - x_k)^{y_k}\}, \eta \geq \eta_o \qquad (11)$$

In the tail region, there is a gradual variation with respect to the function $z_k(\eta)$ as against the exponential function $\exp\{-w_k(\eta - x_k)^{y_k}\}$, therefore the tail marker η_o can replace it.

Furthermore, the constants w, x, y and z can be evaluated by the Levenberg-Marquardt least-squares optimization method. The probability of occurrence of the extreme value can gotten by the ACER method on the bases of the least square's method[29].

3.4 ACER 1D Method

The approximation of extreme value distribution of a given recorded time series in its tail had been carried out by different statistical methods. In the study of wind turbines, some statistical methods used includes an estimation of structural responses in floating vertical axis wind turbines, see [27].

One of the advantages of the ACER method used in this paper as in [30] is the possibility to identify the outcome of dependency from the data of the time series on the extreme value distribution. Furthermore, the entire time series data can be input without de-clustering, meaning there will be no need to use independent data. Nonetheless, the capability to produce a non-parametric characterization of the extreme value distribution inherent in the data is the most outstanding factor of the ACER method. There will therefore be no need for clear-cut modelling because of seasonal effects, given that it is accounted for by the model. The study of vessels extreme roll assessment has been studied recently using the ACER method[31].

3.5 ACER 2D Method

The analysis of the FWT blades due to environmental wind wave loads has been carried out by the ACER2D method. The stochastic response of the blade is time synchronous. To predict high quantiles in the extreme value distribution, which would usually have to do with out of sample predictions, ACER functions must be represented by a unique class of parametric functions[2].

3.6 Load cases and environmental conditions

The wind data used in this paper is based on hindcast data obtained during a 10-year period from site 14 in the Northern North Sea. Lin Li et al.[32] developed the long-term joint wind and wave distribution, where a one-hour mean wind speed 10 meters above sea level (U_{10})was

considered along with wave spectral period (T_p) and significant wave height (H_s). The joint distribution is expressed as:

$$f_{U_{10},H_S,T_P}(u,h,t) = f_{U_{10}}(u) \cdot f_{H_S|U_{10}}(h|u) \cdot f_{T_P|U_{10},H_S}(t|u,h) \tag{12}$$

where $f_{U_{10}}(u), f_{H_S|U_{10}}(h|u)$ and $f_{T_P|U_{10},H_S}(t|u,h)$ expresses the marginal distribution of U_{10}, the conditional distribution of H_s for a given U_{10} and the conditional distribution of T_p for a given U_{10} and H_s. Figure 4 shows H_s and T_p in a scattered diagram, employed to designate probabilities to a given sea state.

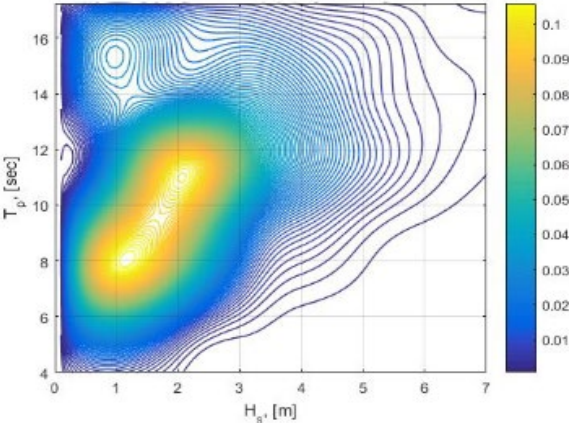Figure 4 Hs and Tp values in scattered diagram for assigning probabilities to respective sea states[32]

Load cases	U_w(m/s)	T_1	H_S(m)	T_P(s)	Samples	Simulation length (s)
LC 1	8	0.1740	1.9	9.7	20	4000
LC 2	12	0.1460	2.5	10.1	20	4000
LC 3	16	0.1320	3.2	10.7	20	4000

Figure 5 Simulation load cases

4. RESPONSE VARIABLES

Figure 5 depicts the 5 locations where the maximum loads with respect to wind accelerations in x, y and z directions are evaluated.
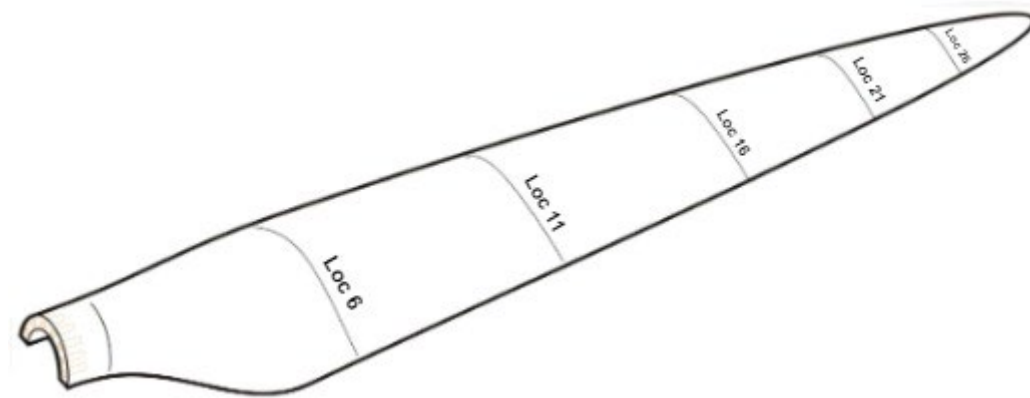

Figure 6 Locations where maximum loads are measured

5. RESULTS AND DISCUSSIONS

The methodology for estimating the extreme loads during parked condition on the 10MW DTU -OO Star is presented in this paper. The wind data used is retrieved from hindcast data obtained during a 10-year period from site 14 in the Northern North Sea as explained in Section 3.4. Extensive use of MATLAB has been employed to post-process the data and calculate the acceleration of the 3 load cases at the 5 respective points in x, y, and z directions. Plots of acceleration vs time on Loc.6 at the load cases, 8, 12 and 16m/s respectively are shown below.

Location 6 @ 8m/s Acceleration/Time Graph

Location 6 @ 12m/s Acceleration/Time Graph
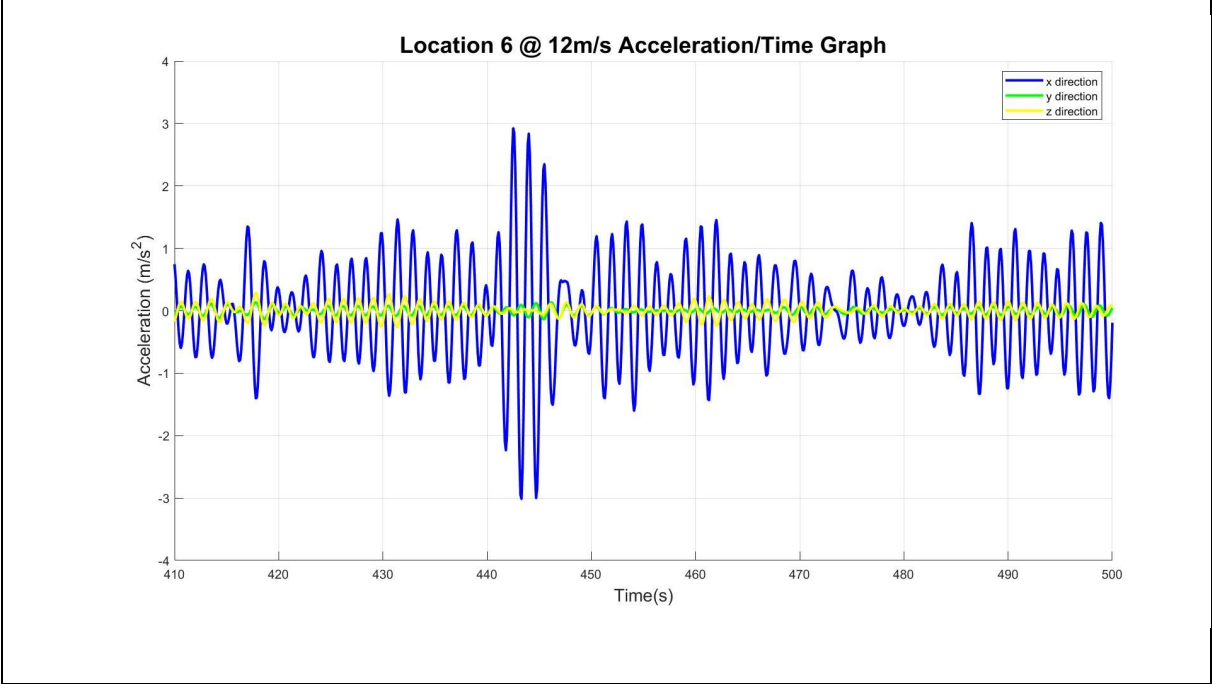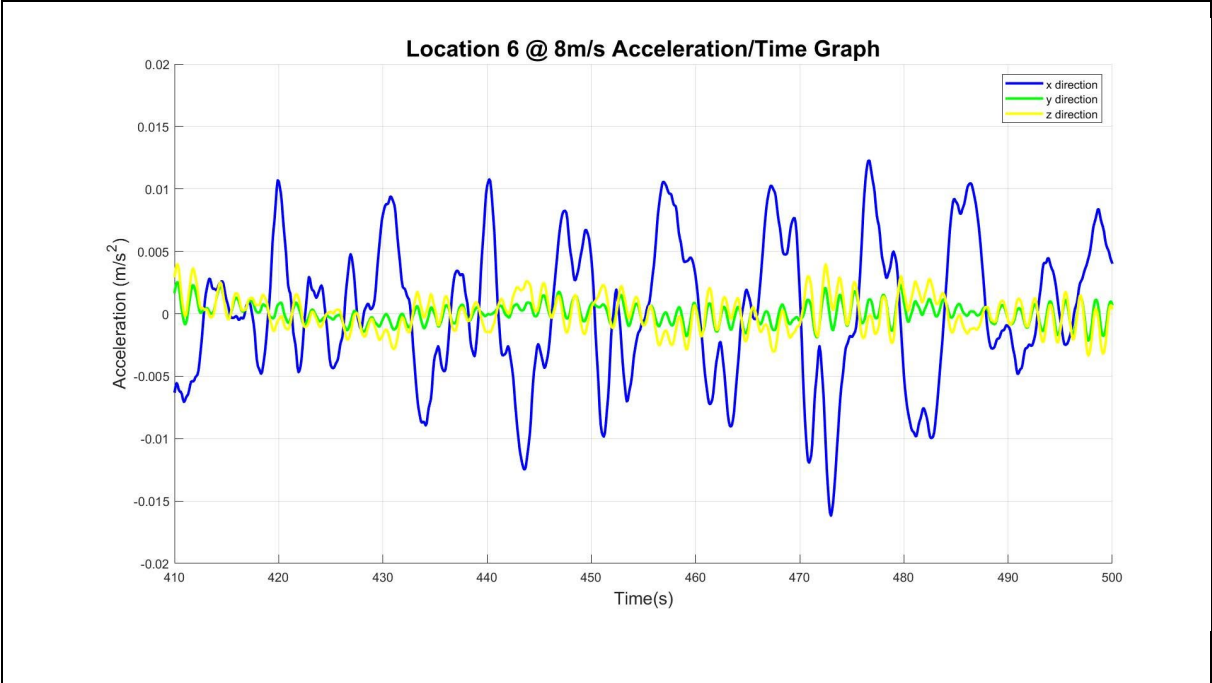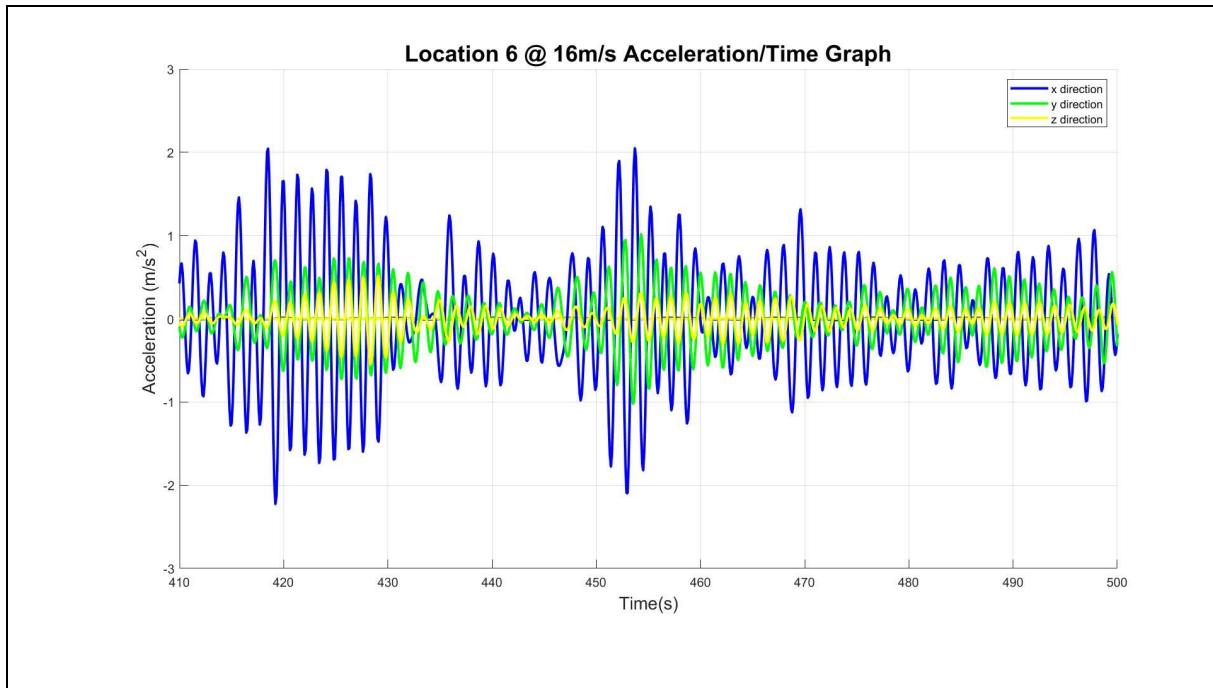
Figure 7 Acceleration vs Time showing higher peaks in Loc. 6 due to increased acceleartion

Figure 7 clearly shows the validity of the post process carried out with MATLAB, because a depiction of higher vibrations is expected due to a an increase in acceleration in same location.

5.1 ACER vs GUMBEL confidence interval results

As described in 3.5, the results from ACER have been compared with the generalized extreme value distribution of Gumbel for the purpose of sampling and comparing the maximum number of samples based on one year return period with a 95% certainty.

The table below shows the numbers for each of the load cases as well as a graph depicting the similarities in values between ACER and GUMBEL.

	8ms				
	loc_6_x	loc_11_x	loc_16_x	loc_21_x	loc_26_x
ACER	0.8981446	-0.255939	-2.1224115	-4.8396943	-5.4932617
GUMBEL	0.34	-0.73	-2.62	-5.37	-6.00

	8ms				
	loc_6_y	loc_11_y	loc_16_y	loc_21_y	loc_26_y
ACER	16.8193979	24.670019	43.672845	69.1850952	75.542213
GUMBEL	14.42	25.14	44.17	72.16	78.51

	8ms				
	loc_6_z	loc_11_z	loc_16_z	loc_21_z	loc_26_z
ACER	-5.959693	-12.07659	-48.298536	-38.82995	-42.435033
GUMBEL	0.34	-0.73	-2.62	-5.37	-6.00

	12ms				
	loc_6_x	loc_11_x	loc_16_x	loc_21_x	loc_26_x
ACER	6.9292564	7.8444875	12.820103	20.355029	22.517937
GUMBEL	6.96	7.81	10.71	15.70	16.89

	12ms				
	loc_6_y	loc_11_y	loc_16_y	loc_21_y	loc_26_y
ACER	125.711242	27.280295	46.536251	74.9827405	-19.68139
GUMBEL	15.38	26.20	45.43	73.87	80.32

	12ms				
	loc_6_z	loc_11_z	loc_16_z	loc_21_z	loc_26_z
ACER	-4.235537	-9.500476	46.536251	-31.22847	-34.164769
GUMBEL	-4.72	-10.26	-19.54	-32.90	-35.92

	16ms				
	loc_6_x	loc_11_x	loc_16_x	loc_21_x	loc_26_x
ACER	-338.9922	6.0937721	12.181385	-18.368462	-31.398571
GUMBEL	5.86	7.61	11.41	18.36	19.95

	16ms				
	loc_6_y	loc_11_y	loc_16_y	loc_21_y	loc_26_y
ACER	11.9705064	22.552074	41.644037	74.7047053	33.782927
GUMBEL	15.12	25.81	44.82	73.44	79.33

	16ms				
	loc_6_z	loc_11_z	loc_16_z	loc_21_z	loc_26_z
ACER	-8.478656	-9.794364	-18.368462	-31.39857	-34.447621
GUMBEL	-5.28	-10.49	-19.73	-33.14	-36.18

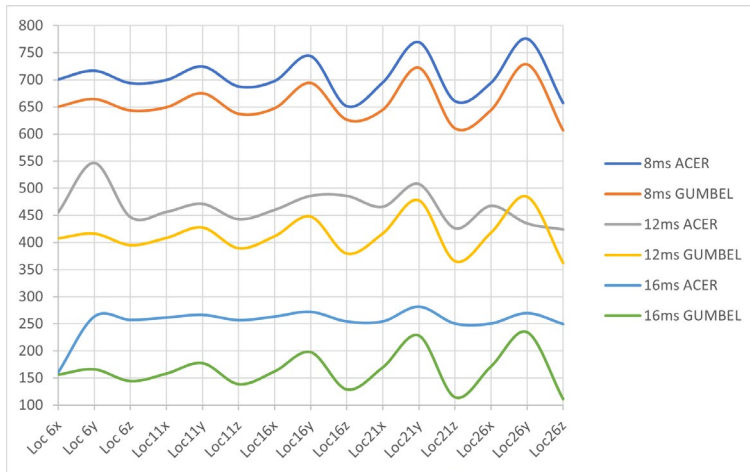Figure 8 Confidence Interval (ACERvsGUMBEL)

Figure 9 Graph showing confidence interval(ACERvsGUMBEL)

5.2 Discussion on confidence interval results

As seen in Figure 9 the ACER and GUMBEL results have similar patterns at all measurement points and directions wind acceleration of $8\mathrm{ms}^{-2}$ but as the acceleration increases to $12\mathrm{ms}^{-2}$ it is found that these patterns become more different and at $16\mathrm{ms}^{-2}$ the ACER results are

relativley far from the GUMBEL results. This suggests that it may be more accurate to analize and draw up conclusions with lower wind accelarations.

Table 5 ACER output results

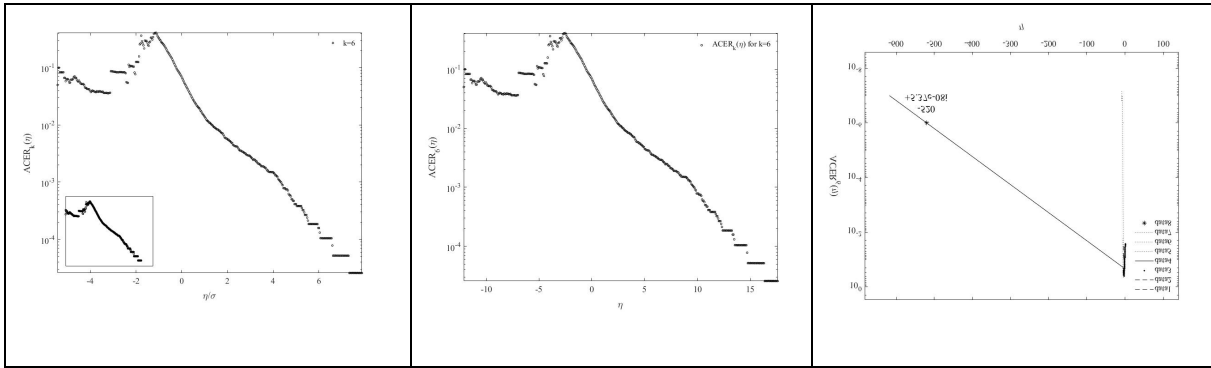| Load Case	Parameters of optimal curve				
	k	q	b	a	c
LC1, x = 8m/s	6	0.256564	-2.5	0.0785546	3.79782
LC2, x= 12m/s	6	2.50515	-8	0.121928	1.64676
LC3, x = 16m/s	6	0.13903	-18.7914	-0.0236318	1
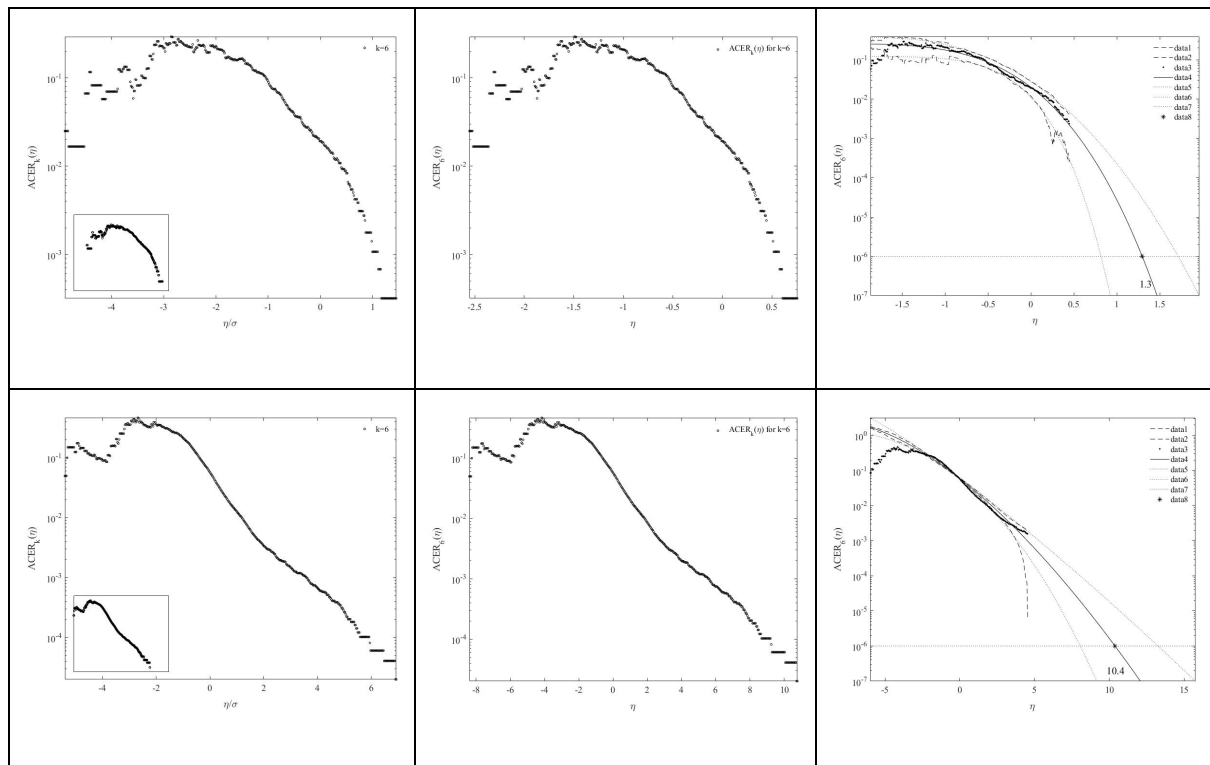
Table 6 ACER functions for k value of 6 for various load cases. Top:LC1, Xdir.=8m/s; Centre: LC2, Xdir.=12m/s; LC3, Xdir.=16m/s

5.3 Discussion on ACER analysis

Through the ACER analysis as decribed earlier, the extraction of peaks as well as the stationarity of the loaded time series were activated. The output results gave the maximum and minimum values of the loaded process, the mean values of the process and the predicted confidence intervals.

5.4 Impact

The methodlogy presented in this report is advantegous such that coupled data can be analyzed irrespective of how it is generated, either measured or simulated.

A correction could be done on the basis of the bivariate statistical analysis for variabes that are correlated to a very high extent, the importance here is that at the design stage . The intent, is to be able to adequately use the data set and create and inclusive design for remotely controlled vehicles that can perform light maintenance repairs on the blades of the wind turbine.

6.0 Conclusion

This research probed into the extreme responses for the blades of a 10MW semi-submesible type FWT employing Gumbel and ACER methods. Contemporary prerequisites in choosing design points by the use of recently developed ACER method have been suggested in this paper. A 10 year hindcast wind-wave data set obtained between 2001-2012 from site 14 in the northern north sea was applied to the bivariate ACER2D method.

In discussing local wind obeservations, an appropraite approach would be the multivariate analysis, quite purposive for practicalities in terms of design route. It is interesting to have studied the impact in analysing data results from both ACER 2D and Gumbel, see Ref.5.1 and to have derived the following:

The ACER results are moderately more and have a reduced 95% CI (Confidence Interval) than the Gumbel results. The extract here is that ACER method is orthodox and more reliable as against the GUMBEL method.

Finally, due to the fact that Gumbel reads the extreme responses as following a designated probability distribution and ACER doesn't, it is concluded that the later has a better execution .

References

[1]   A. Naess and O. Karpa, "Statistics of bivariate extreme wind speeds by the ACER method," *Journal of Wind Engineering and Industrial Aerodynamics,* vol. 139, pp. 82-88, 2015.

[2]   O. G. A. Naess, and O. Karpa, "Estimation of Extreme Values by the Average Conditional

Exceedance Rate Method," *Journal of Probability and Statistics,* Research Article vol. 2013, p. 15, 2013.

[3]   K. S. Wiebe, M. Harsdorff, G. Montt, M. S. Simas, and R. Wood, "Global Circular Economy Scenario in a Multiregional Input-Output Framework," *Environ Sci Technol,* vol. 53, no. 11, pp. 6362-6373, Jun 4 2019, doi: 10.1021/acs.est.9b01208.

[4]   W. Tong, *Wind power generation and wind turbine design*. WIT press, 2010.

[5]   I. R. E. Agency, "Future of wind," *A Global Energy Transformation paper,* vol. EXECUTIVE

SUMMARY, 2019.

[6]   G. L. Kyriakopoulos, "15 - Should low carbon energy technologies be envisaged in the context of sustainable energy systems?," in *Low Carbon Energy Technologies in Sustainable Energy Systems*, G. L. Kyriakopoulos Ed.: Academic Press, 2021, pp. 357-389.

[7]   E. E. Bachynski, "Fixed and Floating Offshore Wind Turbine Support Structures," in *Offshore Wind Energy Technology*, 2018, pp. 103-142.

[8]   P. H. Madsen, " Predicting ultimate loads for wind turbine design (award for best wind energy conference paper 1999)," *Article in proceedings,* 1999.

[9]   N. Dimitrov, "Comparative analysis of methods for modelling the short-term probability distribution of extreme wind turbine loads," *Wind Energy,* vol. 19, no. 4, pp. 717-737, 2016.

[10]   O. Gaidai, F. Wang, Y. Wu, Y. Xing, A. R. Medina, and J. Wang, "Offshore renewable energy site correlated wind-wave statistics," *Probabilistic Engineering Mechanics,* vol. 68, p. 103207, 2022/04/01/ 2022, doi: https://doi.org/10.1016/j.probengmech.2022.103207.

[11]   K. M. Wei Yu, Frank Lemmer, "Qualification of innovative floating substructures for

10MW wind turbines and water depths greater than 50m," *LIFES50+,* 2018.

[12] S. Wang, T. Moan, and A. R. Nejad, "A comparative study of fully coupled and de-coupled methods on dynamic behaviour of floating wind turbine drivetrains," *Renewable Energy,* vol. 179, pp. 1618-1635, 2021.

[13] C. Bak, Zahle, F. , Bitsche, R. , Kim, T. , Yde, A. , Henriksen, L. C. , Hansen, M. H. , Blasques, J. P. A. A. , Gaunaa, M., & Natarajan, A., "The DTU 10-MW Reference Wind Turbine," *Sound/Visual production (digital),* 2013.

[14] S. Wang, T. Moan, and Z. Jiang, "Influence of variability and uncertainty of wind and waves on fatigue damage of a floating wind turbine drivetrain," *Renewable Energy,* vol. 181, pp. 870-897, 2022/01/01/ 2022, doi: https://doi.org/10.1016/j.renene.2021.09.090.

[15] S. Wang, A. R. Nejad, E. E. Bachynski, and T. Moan, "Effects of bedplate flexibility on drivetrain dynamics: Case study of a 10 MW spar type floating wind turbine," *Renewable Energy,* vol. 161, pp. 808-824, 2020.

[16] B. J. Jonkman and M. L. Buhl Jr, "TurbSim user's guide," National Renewable Energy Lab.(NREL), Golden, CO (United States), 2006.

[17] H. Ormberg, E. Passano, and N. Luxcey, "Global analysis of a floating wind turbine using an aero-hydro-elastic model: Part 1—code development and case study," in *International Conference on Offshore Mechanics and Arctic Engineering*, 2011, vol. 44373, pp. 837-847.

[18] N. Luxcey, H. Ormberg, and E. Passano, "Global analysis of a floating wind turbine using an aero-hydro-elastic numerical model: Part 2—benchmark study," in *International Conference on Offshore Mechanics and Arctic Engineering*, 2011, vol. 44373, pp. 819-827.

[19] A. N. Robertson *et al.*, "OC5 Project Phase Ib: Validation of hydrodynamic loading on a fixed, flexible cylinder for offshore wind applications," *Energy Procedia,* vol. 94, pp. 82-101, 2016.

[20] G. Fernandez, H. Usabiaga, and D. Vandepitte, "An efficient procedure for the calculation of the stress distribution in a wind turbine blade under aerodynamic loads," *Journal of Wind Engineering and Industrial Aerodynamics,* vol. 172, pp. 42-54, 2018.

[21] G. Ingram, "Wind turbine blade analysis using the blade element momentum method. version 1.1," *Durham University, Durham,* 2011.

[22] S. Ocean, "RIFLEX 4.10. 3 User Guide," 2017.

[23] C. Lee, "Theory Manual," 1995.

[24] T.-S. Tang and M. Styblinski, "Yield optimization for nondifferentiable density functions using convolution techniques," *IEEE transactions on computer-aided design of integrated circuits and systems,* vol. 7, no. 10, pp. 1053-1067, 1988.

[25] C.-C. Peng and C.-L. Lee, "Performance Demands based Servo Motor Speed Control: A Genetic Algorithm Proportional-Integral Control Parameters Design," 2020: IEEE, pp. 469-472, doi: 10.1109/IS3C50286.2020.00128.

[26] L. Makkonen, "Plotting positions in extreme value analysis," *Journal of Applied Meteorology and Climatology,* vol. 45, no. 2, pp. 334-340, 2006.

[27] Z. Cheng, H. A. Madsen, W. Chai, Z. Gao, and T. Moan, "A comparison of extreme structural responses and fatigue damage of semi-submersible type floating horizontal and vertical axis wind turbines," *Renewable Energy,* vol. 108, pp. 207-219, 2017.

[28] K. Xu, M. Zhang, Y. Shao, Z. Gao, and T. Moan, "Effect of wave nonlinearity on fatigue damage and extreme responses of a semi-submersible floating wind turbine," *Applied Ocean Research,* vol. 91, p. 101879, 2019.

[29] A. Næss and O. Gaidai, "Estimation of extreme values from sampled time series," *Structural safety,* vol. 31, no. 4, pp. 325-334, 2009.

[30] A. Naess, O. Gaidai, and O. Batsevych, "Prediction of extreme response statistics of narrow-band random vibrations," *Journal of engineering mechanics,* vol. 136, no. 3, pp. 290-298, 2010.

[31] X.-s. Xu, O. Gaidai, O. Karpa, J.-l. Wang, R.-c. Ye, and Y. Cheng, "Wind Farm Support Vessel Extreme Roll Assessment While Docking in the Bohai Sea," *China Ocean Engineering,* vol. 35, no. 2, pp. 308-316, 2021.

[32] L. Li, Z. Gao, and T. Moan, "Joint environmental data at five european offshore sites for design of combined wind and wave energy devices," in *International Conference on Offshore Mechanics and Arctic Engineering*, 2013, vol. 55423: American Society of Mechanical Engineers, p. V008T09A006.